

RF SYSTEM EXPERIENCE FOR FRIB HALF WAVE RESONATORS*

S. Zhao†, W. Chang, E. Daykin, E. Gutierrez, S. Kim, S. Kunjir, T. Larter, D. Morris, J. Popielarski,
 Facility for Rare Isotope Beams, Michigan State University, East Lansing, MI, USA

Abstract

The installation and commissioning of the Facility for Rare Isotope Beams (FRIB) superconducting linac adopts a phased strategy. In SRF'19 we reported the progress on the commissioning of the linear segment 1 (LS1) which contains mainly the quarter wave resonators (QWRs). In this paper, we will report the recent progress on the commissioning of the remainder of the linac, including linear segment 2 (LS2), folding segment 2 (FS2) and linear segment 3 (LS3), focusing on the RF system experience for the half wave resonators (HWRs). Compared to the QWRs, the HWRs have a different type of tuner, run at higher power levels and have additional components (for example, high voltage bias tee for multipacting suppression and spark detector). Topics such as nonlinear tuner control for the pneumatic tuners, auto turn on/off implementation, and early issues and failures will be discussed in more detail.

INTRODUCTION

As presented previously, the Facility for Rare Isotopes Beams (FRIB) adopts a phased commissioning strategy [1, 2]. Table 1 shows the FRIB accelerator readiness review (ARR) schedule. The linear segment 1 (LS1) and folding segment 1 (FS1) were commissioned by February 2019 when all quarter wave resonators (QWRs) were commissioned. In the past two year, FRIB has made significant progress on the linac commissioning even under the effect of the COVID-19 pandemic. The ARR4 was completed by March 2020 and ARR5 was completed by April 2021 during which all half wave resonators (HWRs) were successfully commissioned.

Table 1: FRIB ARR Phases

ARR Phase	Area with beam	Energy MeV/u	Date
1	Front end	0.5	07/2017
2	+ $\beta = 0.041$	2	05/2018
3	+ $\beta = 0.085$ (LS1, FS1)	20	02/2019
4	+ $\beta = 0.29, 0.53$ (LS2)	200	03/2020
5	+ $\beta = 0.53$ (FS2, LS3)	>200	04/2021
6	+ target, beam dump	>200	09/2021
Final	integration with NSCL	>200	06/2022

As shown in Table 2, HWRs with 220 cavities in total make up two thirds of the FRIB Linac. Compared to the QWRs, the HWRs have a different type of tuner and run at higher frequency and higher power levels [3]. HWRs also

* Work supported by the U.S. Department of Energy Office of Science under Cooperative Agreement DE-SC0000661.

† zhaos@frib.msu.edu

have additional components such as high voltage bias tee for coupler multipacting (MP) suppression and spark detectors.

Table 2: FRIB Superconducting Cavity Types

Cavity Type	Freq. (MHz)	Power (kW)	Tuner	Qty
$\beta=0.041$ QWR	80.5	0.7	Stepper	12
$\beta=0.085$ QWR	80.5	2.5	Stepper	92
$\beta=0.29$ HWR	322	3.0	Pneumatic	72
$\beta=0.53$ HWR	322	5.0	Pneumatic	148

For the rest part of the paper, several topics that are related to the RF system for the HWRs will be discussed, including resonance control, automation, HWR specific components and issues encountered.

PNEUMATIC TUNER CONTROL

The HWRs use pneumatic tuners in comparison to the stepper tuners used by the QWRs. The pneumatic tuner control has evolved significantly over the years since HWR integrated test, cryomodule bunker test and test in the linac tunnel trying to improve the tuner control performance.

The main challenge can be explained with the valve characteristic curve as shown in Figure 1. First, the valve does not give any flow if the control signal is less than certain amount (typically 30~40%); second, the point where flow begins is uncertain (due to static friction, pressure operating point, thermal effect of the coil in the valve, etc.); third, the flow needed for tuning is less than 15% which means the valve operates mostly in the nonlinear region.

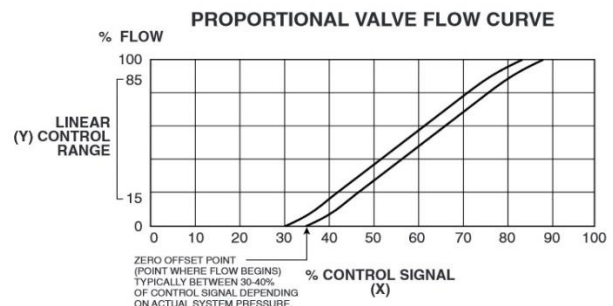


Figure 1: Valve characteristic.

The “static” deadzone mentioned in the first point can be easily addressed by calibrating the valve close voltage (vClose). Due to the uncertainty mentioned in the second point, however, a “dynamic” deadzone of around 10% (or 0.5 V for 0 ~ 5 V control signal) is unavoidable. The maximum flow is limited by calibrating the valve open voltage (vOpen) to around 0.15 ~ 0.2 psi/s which correspond to a maximum cavity tuning rate of 150 ~ 200 Hz/s.

Content from this work may be used under the terms of the CC BY 4.0 licence (© 2022). Any distribution of this work must maintain attribution to the author(s), title of the work, publisher, and DOI

Besides the nonlinearity around the deadzone, the relation between cavity detuning in Hz and detuning measurement in degree is also nonlinear, when detuning is greater than one cavity bandwidth. So a nonlinear control that consists of two nonlinear sections is designed to improve over the standard proportional control as shown in Figure 2.

Nonlinear section 1 allows a small tuner error to generate a relative large control effort to overcome the deadzone quickly. Nonlinear section 2 is used to quickly reduce the flow, i.e. the tuning speed, as cavity gets closer to resonance, preventing oscillation due to overshoot. The two sections are separated by the standard proportional line. The nonlinearity (linear, square root, cubic root, etc.) controls the slope in the middle range (20 ~ 70 degrees). The gain (kp) determines where the two nonlinear sections connect and effectively shifts the curve up or down.

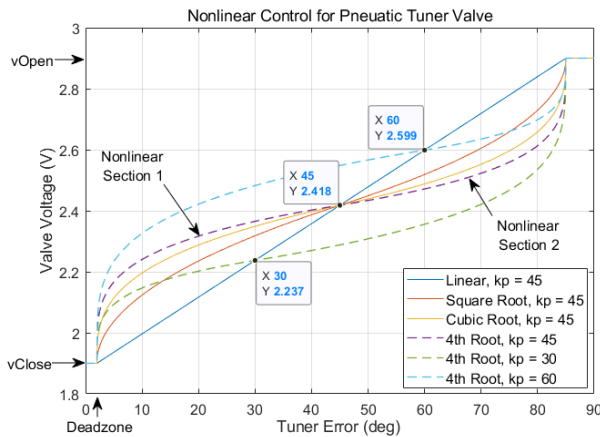


Figure 2: Bias tees installed in FRIB tunnel for HWRs.

For integral control, two integral terms are used, one for each valve. As shown in Figure 3, when the tuner error (absolution value) is greater than the deadzone (usually set to 3 to 5 degrees), the term starts to integrate. The integral term holds its current value when it is within the deadzone. It will start to rewind when the tuner error goes to the other direction (sign flipped). The integral term is bounded between 0 V and 0.5 V.

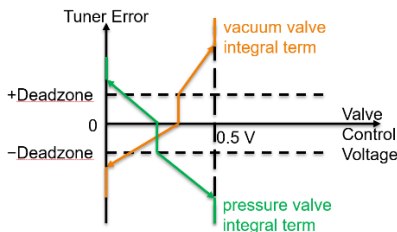


Figure 3: Integration mechanism illustration.

Remark: The nonlinear control method presented above has been proved to be working well and is currently implemented, but before it was validated other alternatives to improve the pneumatic tuner control were investigated [4]. It is also worth to mention that without a simple, reliable resonance control method the automation of cavity turn on process would be harder to implement. That is also why the auto on feature for HWR was not ready until the second beam run of ARR4 in October 2020.

AUTO TURN ON/OFF DEVELOPMENT

To efficiently and reliably operate a large scale facility with over 300 cavities of various types could be very challenging. Automatic turn on procedures have been developed and implemented on the input/output controller (IOC) level for all FRIB cavity types to address this challenge. After resolving the difficulty in pneumatic tuner control, the auto on feature was implemented and tested for the HWRs.

Figure 4 shows a typical HWR auto turn on process. After the auto start command being issued by the operator, the high voltage for the bias tee is turned on and the tuner valves are enabled. The RF drive is enabled at the initial level (1.5 MV/m) afterward, followed by enabling the tuner control. Once the cavity is on resonance, the amplitude control switches to closed-loop and start ramping to the final amplitude set-point. The phase control will switch to closed-loop once final amplitude set-point is reached and the automatic turn on process completes. The whole process takes about 30 seconds. During the first beam run of ARR4 in March 2020, without the auto turn on, each HWR was turned on manually and took about 2 minutes for each cavity.

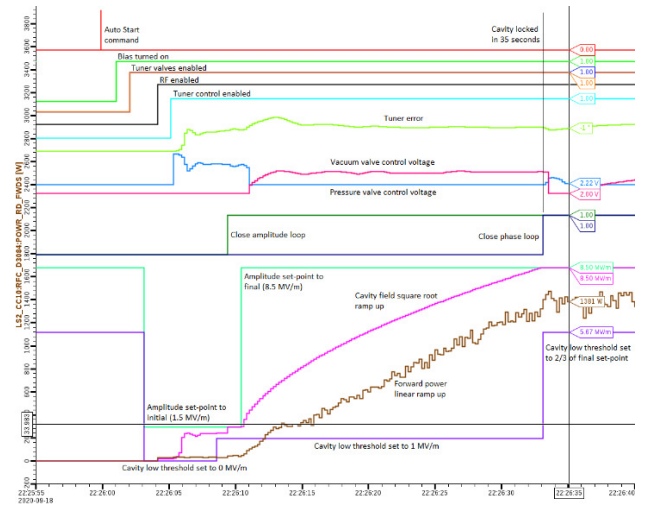


Figure 4: HWR auto turn on process.

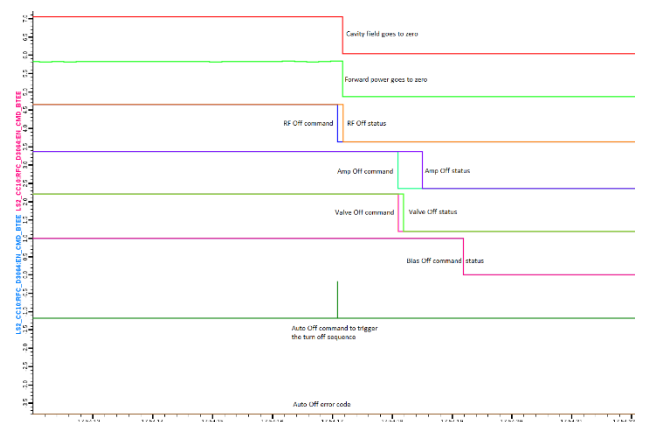


Figure 5: HWR auto turn off process.

Content from this work may be used under the terms of the CC BY 4.0 licence (© 2022). Any distribution of this work must maintain attribution to the author(s), title of the work, publisher, and DOI

The auto turn off process, see Figure 5, is relative simple in comparison to the auto turn on process, but it is still necessary to ensure different components are turned off in the right order and with proper confirmation.

AUTOMATIC MP CONDITIONING

The HWRs have MP barriers at different field levels. The high barrier occurs at around 3 MV/m. Once the high barrier is excited and conditioned, the middle barrier at around 0.1 MV/m is usually observed. A low barrier less than 0.01 MV/m happens in some cases, but it can be jumped over relatively easily and usually does not need to be conditioned.

The MP conditioning is time consuming and labor intensive which motivated us to automate the process. Especially when LS2 was partially warmed up (to 60K) to facilitate some cryogenic work, the HWRs multipacting need to be reconditioned. The automation implementation was tested during LS3 SRF commissioning in January 2021.

As can be seen in Figure 6, power is ramped up while monitoring the X-ray sensor and cavity field. The initial drop of cavity field (red curve) and increasing of X-ray (orange curve) indicate the higher barrier is excited. Then the power is increased very slowly to keep the X-ray level low. After the high barrier is conditioned, it will be rescanned for confirmation. The middle barrier is conditioned usually takes much less time. Then both high barrier and low barriers will be rescanned for confirmation. The whole process takes 20 to 50 minutes depending on cavities.

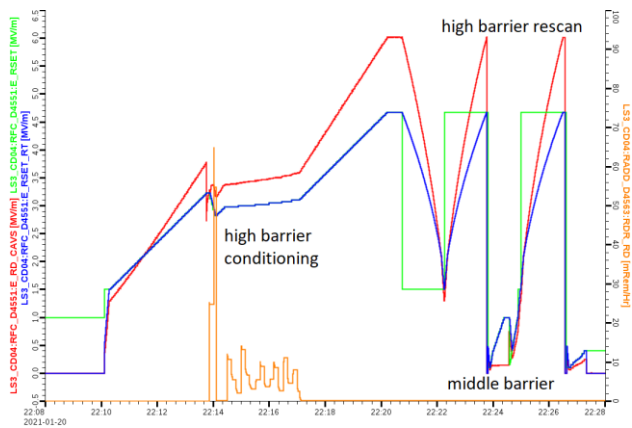


Figure 6: Bias tees installed in FRIB tunnel for HWRs.

Remark: When developing and using the auto MP conditioning tool, extremely care has to be taken. For example, make sure the X-ray sensor is responding. Because any miss handling could cause damage to the cavities.

HWR SPECIFIC COMPONENTS

Due to running at higher power, some additional components are needed for the HWRs compared to the QWRs.

Bias Tee

The FRIB fundamental power coupler (FPC) for the HWRs was designed to minimize the effect of multipacting [5]. But the MP can still occur in certain situations. To reliably suppress the MP in the FPC, a bias tee with high

DC bias voltage (- 1kV) was designed in collaboration with an industrial partner [6], see Figure 7.

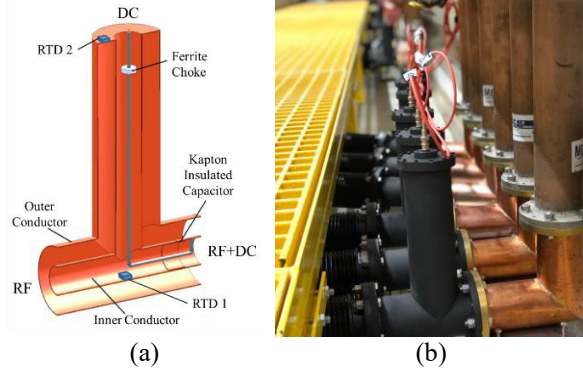


Figure 7: (a) Bias tee conceptual model; (b) Bias tees installed in the FRIB tunnel for HWRs.

The design was iterated several times to reduce the heating on the inner conductor when operating at high power (5 kW). Table 3 shows the temperature data of different revisions.

5 kW Testing	RTD 1: inner junction	RTD 2: short circuit plate
Prototype	78.56 °C	39.00 °C
Rev. A	101.68 °C	42.23 °C
Rev. E	49.10 °C	45.60 °C

Spark Detector

On the FPC a window is available for the purpose of detecting sparks. Due to potential radiation damage, the spark detector circuitry is placed in the rack room rather than in the tunnel. A thick core ($\phi 1.8$ mm) fiber is used to transmit the light from the tunnel to the rack room. The light emitting diode (LED) in the spark detector cup (see Figure 8) is used to perform a roll call test to ensure that the fiber is not clouded or broken and the spark detector circuitry functions normally. If a spark is detected while the cavity is running, the cavity will be interlocked off by the low level radio frequency (LLRF) controller [7].



Figure 8: Spark detector cup.

PHASE JUMPS

During the ARR4 second beam commissioning in October 2020, it was noticed that some of the $\beta=0.29$ HWRs tripped the fast protection system (FPS) at the same time due to phase error exceeding ± 1 degree, see Figure 9. Later it was confirmed that all $\beta=0.29$ HWRs (LS2 CC) had phase jumps at the same time, while other parts (QWRs

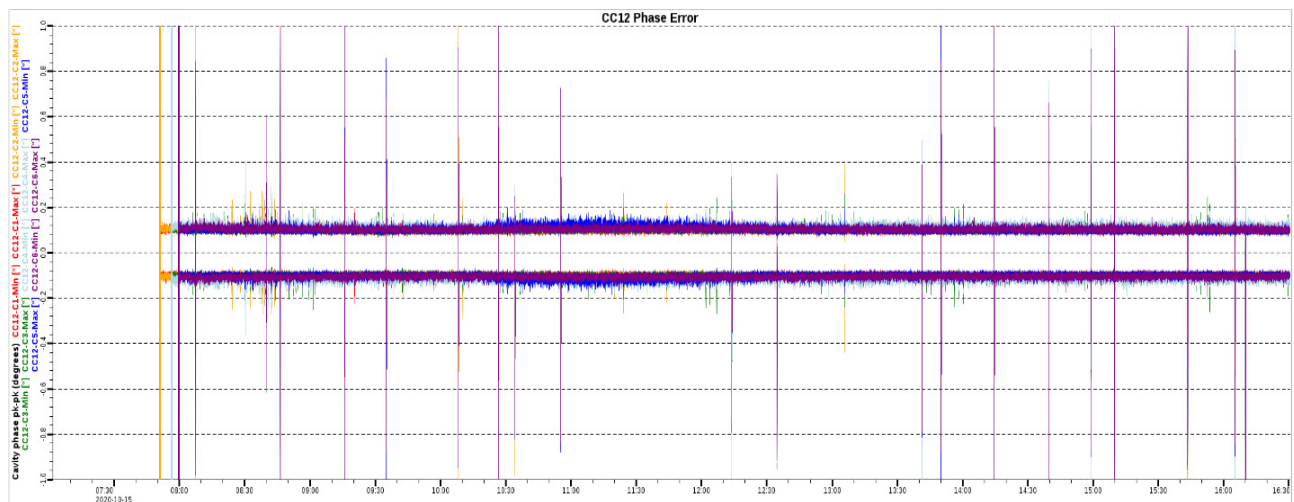


Figure 9: Correlated phase jumps in the last $\beta=0.29$ cryomodule.

and $\beta=0.53$ HWRs) of the linac were not affected. After extensive data collection, cross checking and debugging, the issue was finally resolved in December 2020. The culprit turns out to be a bad connection at the six-way splitter for the reference clock distribution as shown in Figure 10.

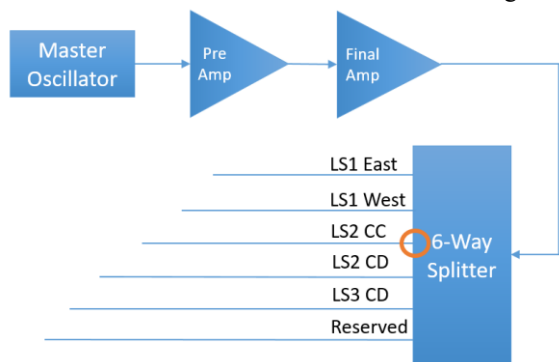


Figure 10: FRIB reference clock distribution diagram.

SUMMARY

Overall the FRIB HWR commissioning was successful despite some challenges and issues. As shown, a lot of effort has been put into the area of automation, which is important for the reliable and efficient operation of FRIB linac. Much more remains to be done. For example, an automatic valve calibration Python script is currently under development for the HWRs, and will be included in the FRIB LLRF Python based tools [8]. More generally for all FRIB cavity types, interlock event auto reporting with fast post-mortem data analysis [9] and real time cavity performance (minimum/maximum error and standard deviation) monitoring could also add value, which will be the tasks in the next step.

REFERENCES

- [1] J. Wei *et al.*, “The FRIB SC-Linac: installation and phased commissioning”, in *Proc. 19th Int. Conf. RF Superconductivity (SRF’19)*, Dresden, Germany, Jun.-Jul. 2019, pp. 12-20. doi:10.18429/JACoW-SRF2019-MOFAA3
- [2] H. Ao *et al.*, “FRIB driver linac integration to be ready for phased beam commissioning”, in *Proc. North American Particle Accelerator Conf. (NAPAC’19)*, Lansing, MI, USA, Sep. 2019, pp. 823-826. doi:10.18429/JACoW-NAPAC2019-WEPLH09
- [3] D. G. Morris *et al.*, “RF System for FRIB Accelerator”, in *Proc. 9th Int. Particle Accelerator Conf. (IPAC’18)*, Vancouver, Canada, Apr.-May 2018, pp. 1765-1770. doi:10.18429/JACoW-IPAC2018-WEXGBF3
- [4] W. Chang *et al.*, “Enhanced pneumatic tuner control for FRIB half wave resonators”, presented at the *20th Int. Conf. on RF Superconductivity (SRF’21)*, Virtual Conference, June 2021, paper THPTEV002, this conference.
- [5] Z. Zheng *et al.*, “Design and Commissioning of FRIB Multipacting-Free Fundamental Power Coupler”, in *Proc. 28th Linear Accelerator Conf. (LINAC’16)*, East Lansing, MI, USA, Sep. 2016, pp. 767-769. doi:10.18429/JACoW-LINAC2016-THOP10
- [6] T. Larter *et al.*, “Design and Implementation of a Production Model Bias Tee”, presented at the *12th Int. Particle Accelerator Conf. (IPAC’21)*, Campinas, Brazil, May 2021. doi:10.18429/JACoW-IPAC2021-TUPAB355
- [7] S. Zhao *et al.*, “The LLRF Control Design and Validation at FRIB”, in *Proc. North American Particle Accelerator Conf. (NAPAC’19)*, Lansing, MI, USA, Sep. 2019, pp.667-669. doi:10.18429/JACoW-NAPAC2019-WEPLM03
- [8] S. Kunjir *et al.*, “Python Based Tools for FRIB LLRF Operation and Management”, presented at the *12th Int. Particle Accelerator Conf. (IPAC’21)*, Campinas, Brazil, May 2021. doi:10.18429/JACoW-IPAC2021-WEPAB300
- [9] S. Zhao *et al.*, “Waveform feature implementation for FRIB LLRF controllers”, in *Proc. LLRF Workshop 2019*, Chicago, IL, USA, Sep.-Oct. 2019. arXiv:1910.06913